

RESEARCH ARTICLES

Open Access



A novel method to calculate compliance and airway resistance in ventilated patients

Guillermo Gutierrez*

*Correspondence:
gutier@gwu.edu

Professor Emeritus Medicine,
Anesthesiology and Engineering,
The George Washington
University, 700 New Hampshire
Ave, NW, Suite 510, Washington,
DC 20037, USA

Abstract

Background: The respiratory system's static compliance (C_{rs}) and airway resistance (R_{rs}) are measured during an end-inspiratory hold on volume-controlled ventilation (static method). A numerical algorithm is presented to calculate C_{rs} and R_{rs} during volume-controlled ventilation on a breath-by-breath basis not requiring an end-inspiratory hold (dynamic method).

Methods: The dynamic method combines a numerical solution of the equation of motion of the respiratory system with frequency analysis of airway signals. The method was validated experimentally with a one-liter test lung using 300 mL and 400 mL tidal volumes. It also was validated clinically using airway signals sampled at 32.25 Hz stored in a historical database as 131.1-s-long epochs. There were 15 patients in the database having epochs on volume-controlled ventilation with breaths displaying end-inspiratory holds. This allowed for the reliable calculation of paired C_{rs} and R_{rs} values using both static and dynamic methods. Epoch mean values for C_{rs} and R_{rs} were assessed by both methods and compared in aggregate form and individually for each patient in the study with Pearson's R^2 and Bland–Altman analysis. Figures are shown as median[IQR].

Results: Experimental method differences in 880 simulated breaths were 0.3[0.2,0.4] mL·cmH₂O⁻¹ for C_{rs} and 0[− 0.2,0.2] cmH₂O·s·L⁻¹ for R_{rs} . Clinical testing included 78,371 breaths found in 3174 epochs meeting criteria with 24[21,30] breaths per epoch. For the aggregate data, Pearson's R^2 were 0.99 and 0.94 for C_{rs} and R_{rs} , respectively. Bias ± 95% limits of agreement (LOA) were 0.2 ± 1.6 mL·cmH₂O⁻¹ for C_{rs} and − 0.2 ± 1.5 cmH₂O·s·L⁻¹ for R_{rs} . Bias ± LOA median values for individual patients were 0.6[− 0.2, 1.4] ± 0.9[0.8, 1.2] mL·cmH₂O⁻¹ for C_{rs} and − 0.1[− 0.3, 0.2] ± 0.8[0.5, 1.2] cmH₂O·s·L⁻¹ for R_{rs} .

Discussion: Experimental and clinical testing produced equivalent paired measurements of C_{rs} and R_{rs} by the dynamic and static methods under the conditions tested.

Conclusions: These findings support to the possibility of using the dynamic method in continuously monitoring respiratory system mechanics in patients on ventilatory support with volume-controlled ventilation.

Keywords: Mechanical ventilation, Acute respiratory failure, Static compliance, Airway resistance, Numerical analysis, Frequency analysis

The respiratory system (rs) static compliance (C_{rs}) and airway resistance (R_{rs}) are calculated during volume-controlled (VC) mechanical ventilation with a breath-hold maneuver at the end of quiet inspiration (static method) [1]. Under these conditions $C_{rs} = V_{\text{tidal}} / (P_{\text{plateau}} - \text{PEEP}_a)$, where V_{tidal} = tidal volume, P_{plateau} = breath-hold P_{aw} , and PEEP_a = applied positive end expiratory pressure. Similarly, $R_{rs} = (P_{\text{peak}} - P_{\text{plateau}}) / F_{\text{aw}}$, where P_{peak} = peak inspiratory pressure and F_{aw} is airway flow measured just prior to breath-holding [2].

A reliable method to calculate C_{rs} and R_{rs} automatically, without the need of an inspiratory hold, would have great utility in monitoring the adequacy of ventilatory support. One approach previously tried is the multiple least squares fit (LSF) technique [3, 4], where measures of P_{aw} , F_{aw} , and lung volume change (ΔV) are fitted to the equation of motion of the respiratory system. Another is the expiratory time constant method [5] where equations for C_{rs} and R_{rs} are developed assuming mono-exponential lung volume release [6]. Both methods require the use of complex computational techniques and absent respiratory muscle effort.

Described is a method to calculate C_{rs} and R_{rs} during insufflation in the presence of airflow (dynamic method) that combines frequency analysis of the airway signals with a novel numerical solution of the equation of motion. The method was validated experimentally with a one-liter test lung. It was also validated clinically using previously acquired F_{aw} and P_{aw} signal data from patients on VC ventilation displaying end-inspiratory holds. This allowed for the reliable calculation of paired C_{rs} and R_{rs} values using both static and dynamic methods.

Theoretical development. The time-dependent equation of motion of the respiratory system is:

$$P_{\text{aw}}(t) = P_{\text{mus}}(t) + P_{\text{vent}}(t) = \frac{\Delta V(t)}{C_{rs}} + R_{rs}F_{\text{aw}}(t) + I \frac{d^2 V(t)}{dt^2} + \text{PEEP}_a + \text{PEEP}_i \quad (1)$$

This equation, based on the one-compartment model of Otis et al. [7], assumes constant values for C_{rs} and R_{rs} . The measured airway pressure $P_{\text{aw}}(t)$ represents the sum of the ventilator and respiratory muscles applied pressures $P_{\text{vent}}(t)$ and $P_{\text{mus}}(t)$, respectively. Opposing them are the elastic, resistive, and inertial components of the respiratory system. $V(t)$ represents the time-dependent lung volume; $\Delta V(t)$ is the insufflation lung volume at time t , equal to $\int_0^t F_{\text{aw}}(t) dt$; I is the respiratory system inertia; and PEEP_i the intrinsic PEEP [8].

Assuming passive insufflation ($P_{\text{mus}} = 0$), negligible PEEP_i , and ignoring the effect of the inertia term [9], Eq. (1) becomes:

$$P_{\text{aw}}(t) = P_{\text{vent}}(t) = \frac{\Delta V(t)}{C_{rs}} + R_{rs}F_{\text{aw}}(t) + \text{PEEP}_a. \quad (2)$$

It is possible to solve numerically this indeterminate equation with two unknowns, C_{rs} and R_{rs} , by first developing a solution matrix for each set of $P_{\text{aw}}(t_k)$, $\Delta V(t_k)$, $F_{\text{aw}}(t_k)$, and PEEP_a values measured at successive times t_k during insufflation. The elements of the solution matrix are calculated by substituting the measured values for $\Delta V(t_k)$,

$F_{aw}(t_k)$, and $PEEP_a$ into Eq. 2 and alternately applying a range of physiologically plausible values for C_{rs} ($C_1 \dots C_n$) and R_{rs} ($R_1 \dots R_n$).

$$\begin{matrix} & R_1 & R_2 & \dots & R_n \\ \text{Solution matrix} = & \begin{bmatrix} P_{aw}(R_1, C_1) & P_{aw}(R_2, C_1) & \dots & P_{aw}(R_n, C_1) \\ \vdots & \vdots & \dots & \vdots \\ P_{aw}(R_1, C_n) & P_{aw}(R_2, C_n) & \dots & P_{aw}(R_n, C_n) \end{bmatrix} & \begin{matrix} C_1 \\ \vdots \\ C_n \end{matrix} \end{matrix}$$

For example, applying a range of ($C_1 \dots C_n$) values from 10 to 100 mL·cmH₂O⁻¹ and 1.0 to 50.0 cmH₂O·s·L⁻¹ for ($R_1 \dots R_n$), at intervals of 0.1 each, produces a 900 × 490 solution matrix containing all possible P_{aw} values capable of satisfying Eq. 2 for given a set of (t_k), $F_{aw}(t_k)$, and $PEEP_a$ measurements made at time t_k during insufflation.

Figure 1 shows a schematic of the proposed numerical method of solution. In this example, a solution matrix was generated for $\Delta V(t_k) = 300$ mL, $F_{aw}(t_k) = 32$ L·min⁻¹, and $PEEP_a = 5$ cmH₂O and plotted as a three-dimensional surface in a Cartesian (C_{rs} , R_{rs} , P_{aw}) system. According to the above reasoning, the solution of Eq. 2, in terms of C_{rs} and R_{rs} , resides on a point on that surface. Further insight is gained by noting that the solution must lie along a surface path traced by the measured $P_{aw}(t_k)$ at time t_k . This is shown in Fig. 1 as path A, where $P_{aw}(t_k) = 27$ cmH₂O and point 'a' symbolizes the yet unknown solution of Eq. 2.

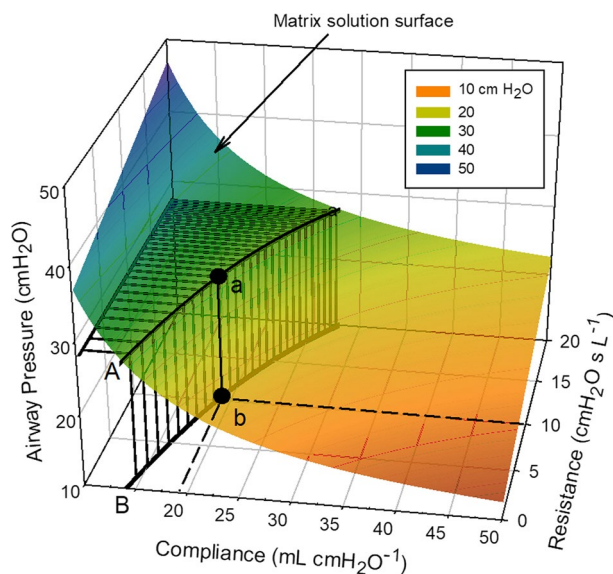


Fig. 1 Schematic of the numerical method used to solve the respiratory system equation of motion for static compliance (C_{rs}) and airway resistance (R_{rs}). In this example, the solution matrix was developed for $\Delta V(t_k) = 300$ mL, $F_{aw}(t_k) = 32$ L·min⁻¹, and $PEEP_a = 5$ cmH₂O and shown graphically as a three-dimensional surface bounded by C_{rs} values ranging from 10 to 50 mL·cmH₂O⁻¹ and R_{rs} from 0 to 20 cmH₂O·s·L⁻¹. This surface encompasses all possible combinations of P_{aw} , C_{rs} and R_{rs} capable of satisfying Eq. 2 for a given set of ΔV , F_{aw} , and $PEEP_a$ measurements made at time t_k during insufflation. P_{aw} also measured at t_k and equal in this example to 27 cmH₂O, further restricts the solution of Eq. 2 to lie along path (A). This path is defined by surface values coinciding with the measured P_{aw} , with point 'a' referring to the still unknown solution of Eq. 2. Projecting path A onto the $C_{rs} - R_{rs}$ plane results in a two-dimensional function (B) relating C_{rs} to R_{rs} . Here 'b' represents the unique solution of Eq. 2 defining the values for C_{rs} and R_{rs} for the breath under consideration

Projecting path (A) onto the C_{rs} - R_{rs} plane generates a two-dimensional function, shown as path B, that restricts all possible combinations of C_{rs} and R_{rs} able to satisfy Eq. 2 for the set of measurements taken at time t_k . The C_{rs} - R_{rs} function is developed numerically by noting the values R_x , C_y associated with those matrix elements where $P_{aw}(R_x, C_y) = \text{measured } P_{aw}(t_k)$.

It only remains to identify the location of solution point 'b' on the C_{rs} - R_{rs} plane. This is accomplished by generating a family of C_{rs} - R_{rs} functions, one for each set of $P_{aw}(t_k)$, $\Delta V(t_k)$, $F_{aw}(t_k)$, and PEEP_a values measured at sequential times t_k during insufflation. Since the one-compartment model of Eq. 2 assumes constant C_{rs} and R_{rs} , it follows that all generated C_{rs} - R_{rs} functions must pass through, and therefore intersect, at a point that defines C_{rs} and R_{rs} for the breath in question.

It is known that C_{rs} and R_{rs} vary early in inspiration as unstable alveoli open and conducting airways distend [10]. However, as lung volume increases past a lower inflection point (LIP) C_{rs} achieves steady state until reaching an upper inflection point (UIP) where over-distention might occur. Defining the LIP and UIP by their respective lung volumes as ΔV_{LIP} and ΔV_{UIP} , it is reasonable to expect all C_{rs} - R_{rs} functions generated for insufflation lung volumes $\Delta V_{LIP} < \Delta V(t) < \Delta V_{UIP}$ to intersect at the solution point 'b' uniquely defining C_{rs} and R_{rs} for that breath.

Figure 2 shows a family of C_{rs} - R_{rs} functions ($n=14$) generated during a single breath's insufflation at sequential 32-ms intervals, past $\Delta V_{LIP} > 200$ mL. The intersection of these functions defines the values for $C_{rs} = 32.8$ mL·cmH₂O⁻¹ and $R_{rs} = 23.8$ cmH₂O·s·L⁻¹. The inset graph illustrates the slight uncertainty associated in determining the intersection of the C_{rs} - R_{rs} functions, likely the result of random variations in measurement or small changes in C_{rs} and R_{rs} occurring during the insufflation. Accordingly, the point of intersection is best defined by the smallest standard deviation (σ) of all C_{rs} values measured at each R_{rs} increment along the R_{rs} axis.

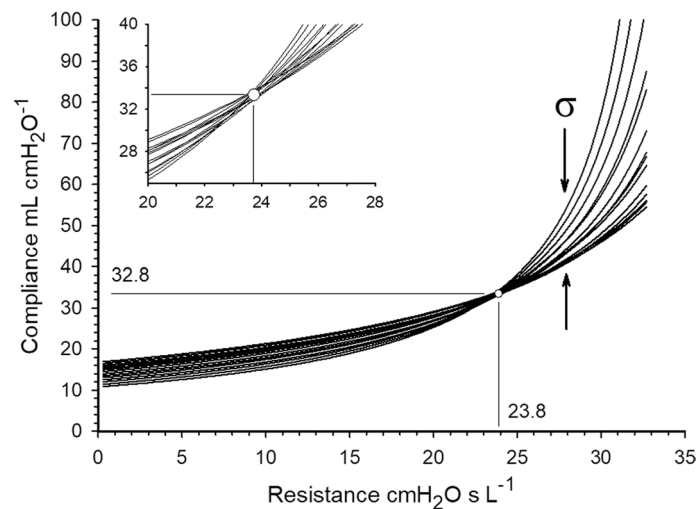


Fig. 2 A family of C_{rs} and R_{rs} functions ($n=14$). Each function was generated at different times (t_k) measured sequentially at 32 ms during a single insufflation. The intersection of these functions defines $C_{rs} = 32.8$ mL·cmH₂O⁻¹ and $R_{rs} = 23.8$ cmH₂O·s·L⁻¹ for the breath. Shown in the inset graph is the uncertainty associated with the intersection point, likely the result of measurement limitations or minute alterations in C_{rs} and R_{rs} during insufflation. Accordingly, the point of intersection is best defined by the smallest standard deviation (σ) of all C_{rs} values measured at each R_{rs} increment along the R_{rs} axis

Methods

The accuracy of the dynamic method was tested by comparing paired C_{rs} and R_{rs} values predicted by the dynamic method and the static method (used here as the 'gold standard') for the same breath.

Experimental validation

Validation was performed experimentally with a Maquet 190 one-liter test lung (Getinge, Solna, Sweden) using VC ventilation with a 0.5-s inspiratory hold. The test lung was attached to a Servo s ventilator (Getinge, Solna, Sweden) and ventilated at a respiratory rate of 15 bpm with V_{tidal} of 300 mL or 400 mL. PEEP levels of 0, 5 and 10 cmH₂O were applied sequentially at each V_{tidal} .

An in-house built data acquisition monitor was used to sample F_{aw} and P_{aw} signals from the ventilator data-port at 32.25 Hz and compile successive epochs of 4096 points, each lasting 131.1 s. Five epochs were obtained at each V_{tidal} -PEEP combination. Data were analyzed in situ with the monitor's Raspberry Pi 3B processor programmed (Python 3.8) to calculate C_{rs} and R_{rs} for each breath by the dynamic method. C_{rs} and R_{rs} were also determined manually by the static method for 10 breaths in each epoch using data from the P_{aw} and F_{aw} signals. Average epoch values for C_{rs} and R_{rs} computed with either method were compared at each V_{tidal} -PEEP combination.

Clinical validation

The dynamic method also was validated with clinical data using F_{aw} and P_{aw} signals obtained in a prior study of mechanically ventilated patients performed in 2011–2012 at The George Washington University Hospital Intensive Care Unit (IRB No. 110910) [11]. The database (Additional file 1: Section S1) contains information from 176 patients with acute respiratory failure enrolled within 24 h of intubation and monitored during their entire time on ventilatory support. It contains deidentified demographic information and F_{aw} and P_{aw} signals sampled at 32.25 Hz by the ventilator (Servo I or Servo S ventilators, Getinge, Solna, Sweden). The signals were saved as contiguous time-windows or epochs, each lasting 131.1 s and containing 4096 samples of each signal.

Epoch selection

Software was written (Python 3.8) to search the database for epochs on VC ventilation. The respiratory rate variability (RRV) for each identified epoch was used to determine the degree of active respiratory muscle activity. RRV was determined from the frequency spectrum of the expiratory flow signal as previously described [12] using the fast Fourier transform (FFT) algorithm [13]. RRV was defined as $100 - H1/DC$ %, where H1 is the amplitude of the spectrum's first harmonic and DC that of the zero-frequency component. Epochs with $RRV < 55\%$ were assumed to have negligible respiratory muscle activity ($P_{mus} = 0$) and were chosen for the study. This RRV value corresponds to those noted in normal individuals during quiet breathing in stages N2 and N3 of sleep [14].

Breath selection

Within each selected epoch, the software further identified breaths displaying an end-inspiratory hold and absent voluntary respiratory effort. These breaths allowed for the reliable measurements of static compliance and airway resistance using standard calculations for comparison with those predicted by the dynamic method. The following criteria was used to choose breaths for analysis: (1) a discernible end-inspiratory hold > 0.25 s with mean plateau airway flow < 1 L·min⁻¹; (2) ventilator-triggered ($PEEP_a - \text{minimal } P_{aw} < 0.3$ cmH₂O); (3) full volume breaths ($\Delta V(t) \geq 300$ mL with insufflation time (Ti) > 0.8 s); (4) absent PEEP_i (end-exhalation (EE) $F_{aw} < 3$ L·min⁻¹ [15] and $P_{aw}(t_0) - EE P_{aw} < 2$ cmH₂O) [16]; and (5) no air circuit leak (inspired – expired $V_{tidal} < |30$ mL). Excluded were breaths with $\Delta V(t) \geq 740$ mL to avoid exceeding the UIP [17] (see Additional file 1: Section S2 for breath exclusion example). Once a breath was deemed adequate for analysis, the software calculated C_{rs} and R_{rs} by both the dynamic and static methods.

Results from the dynamic and static methods were compared with Pearson's linear regression R^2 and Bland–Altman analysis [18] for bias $\pm 95\%$ limits of agreement (LOA). Since some patients had substantially more epochs meeting study criteria than others, the methods were compared in aggregate by combining data from all epochs and individually for each study patient. Unless otherwise specified, data are shown as median and interquartile range. The Mann–Whitney test was used to determine significant differences between independent samples. All reported p values are two-sided with $p < 0.05$ considered significant.

Results

Experimental validation

Analysis of 880 breaths from 30 epochs resulted in nearly identical values for C_{rs} and R_{rs} calculated by the static and dynamic methods for all tested combinations of V_{tidal} and PEEP (Table 1; $p = \text{NS}$). Overall method differences were $0.3[0.2,0.4]$ mL·cmH₂O⁻¹ for C_{rs} and $0[-0.2,0.2]$ cmH₂O·s·L⁻¹ for R_{rs} .

Table 1 Respiratory system's static compliance and resistance values calculated by the static and dynamic methods using a test lung

| V_{tidal} mL | PEEP* cmH ₂ O | Compliance mL·cmH ₂ O ⁻¹ | | Resistance cmH ₂ O·s·L ⁻¹ | |
|-------------------------|-----------------------------|--|-----------------|---|-----------------|
| | | Static | Dynamic | Static | Dynamic |
| 300 | 0 | 21.0[21.0,21.0] | 21.5[21.4,21.5] | 7.9[7.9,8.0] | 7.7[7.6,7.8] |
| | 5 | 22.8[22.8,22.9] | 23.2[23.1,23.3] | 8.2[5.2,8.3] | 8.3[8.2,8.3] |
| | 10 | 26.1[26.0,26.1] | 26.4[26.4,26.3] | 8.2[7.9,8.2] | 8.1[8.1,8.3] |
| 400 | 0 | 22.9[22.9,23.0] | 23.0[23.0,23.1] | 10.5[10.4,10.5] | 10.1[10.0,10.1] |
| | 5 | 24.4[24.4,24.5] | 24.7[24.6,24.8] | 10.7[10.7,10.8] | 11.0[11.0,11.0] |
| | 10 | 27.7[27.7,27.8] | 28.1[28.0,28.1] | 10.7[10.7,11.1] | 11.0[10.9,11.0] |
| Total (n = 880) | | 23.6[22.8,26.1] | 23.9[23.0,26.4] | 9.3[8.2,10.7] | 9.2[8.1,10.9] |
| Difference [†] | | 0.3 [0.2,0.4] | | 0 [-0.2,0.2] | |

There were no significant differences between methods in any of the variables measured

V_{tidal} tidal volume, PEEP positive end expiratory pressure; values shown as median [IQR]

* Five epochs per PEEP level, each containing approximately 30 breaths

† Difference = dynamic – static methods

Clinical validation

Of the 176 patients in the database, 15 (8.5%) were identified as meeting study criteria. The 15 patients had a combined total of 33,371 epochs on VC ventilation and $RRV < 55\%$. The study patients were evenly split according to gender, but ranged widely in age, predicted body weight (PBW) and body mass index (BMI). Disease acuity was high (SAPS II 36[32,44]), five were non-cardiac post-operative, two were trauma and the remainder medical patients. The P/F ratio was relatively high at 337[272,429] mmH_2O , reflecting the lack of lung pathology noted in half of the patients' chest radiographs (Additional file 1: Table S1, Additional file 2, Additional file 3, Additional file 4).

Of the 33,371 identified epochs, 3174 (9.5%) contained breaths displaying end-inspiratory holds. The ventilatory parameters associated with these epochs were compatible with those of quiet, passive ventilation with a low $RR = 11[11,14]$ bpm and $RRV = 45[40,46]\%$ (Additional file 1: Table S2). The 3174 chosen epochs encompassed 87,021 individual breaths with 78,371 (90.1%) considered adequate for analysis of static compliance and airway resistance using standard calculations for comparison with those predicted by the dynamic method. The median number of breaths in these epochs was 24[21,30].

Aggregate data analysis

There was an excellent correlation between the static and dynamic methods (Fig. 3) with $(C_{rs})_{\text{stat}} = 1.06 (C_{rs})_{\text{dyn}} - 2.26$; $R^2 = 0.99$; $p < 0.001$ and $(R_{rs})_{\text{stat}} = 0.93 (R_{rs})_{\text{dyn}} + 1.02$; $R^2 = 0.94$; $p < 0.001$. Bland–Altman analysis (Fig. 4) showed bias \pm LOA of $0.2 \pm 1.6 \text{ mL}\cdot\text{cmH}_2\text{O}^{-1}$ for C_{rs} and $-.2 \pm 1.5 \text{ cmH}_2\text{O}\cdot\text{s}\cdot\text{L}^{-1}$ for R_{rs} .

Individual patient analysis. Table 2 shows Bland–Altman analyses for individual study patients. There were 119 [34, 339] (range 15 to 881) epochs per patient containing 2926 [624, 7702] (range 426 to 17,953) breaths. Individual patient bias \pm LOA for C_{rs} was $0.6 [-0.2, 1.4]$ (range -0.8 to 1.6) $\pm 0.9 [0.8, 1.2]$ (range 0.7 to 2.3) $\text{mL}\cdot\text{cmH}_2\text{O}^{-1}$. Bias \pm LOA for R_{rs} was $-0.1 [-0.3, 0.2]$ (range -1.6 to 2.1) $\pm 0.8 [0.5, 1.2]$ (range 0.2 to 2.2) $\text{cmH}_2\text{O}\cdot\text{s}\cdot\text{L}^{-1}$.

Discussion

Increases in computing power [19] allow for the application of powerful analytical techniques to monitor patients on ventilatory support. The present study describes an algorithm capable of providing breath-by-breath measures of C_{rs} and R_{rs} without the need for an end-inspiratory pause in patients on VC ventilation. This technique may in turn allow for the continuous monitoring of other parameters, such as the driving pressure, a proven indicator of ventilator associated lung injury [20].

The dynamic method used to determine static C_{rs} and R_{rs} is based on a novel numerical solution of the equation of motion of the respiratory system. This equation depicts the behavior of respiratory mechanics in normal individuals and has been applied successfully to ventilated patients with respiratory failure [21]. In the form used here, the equation of motion ignores the inspired gas inertia and the resistance to energy transfer by visco-elastic lung tissue, whereas both terms may be quantitatively significant under extreme ventilatory conditions, they are likely inconsequential under the studied

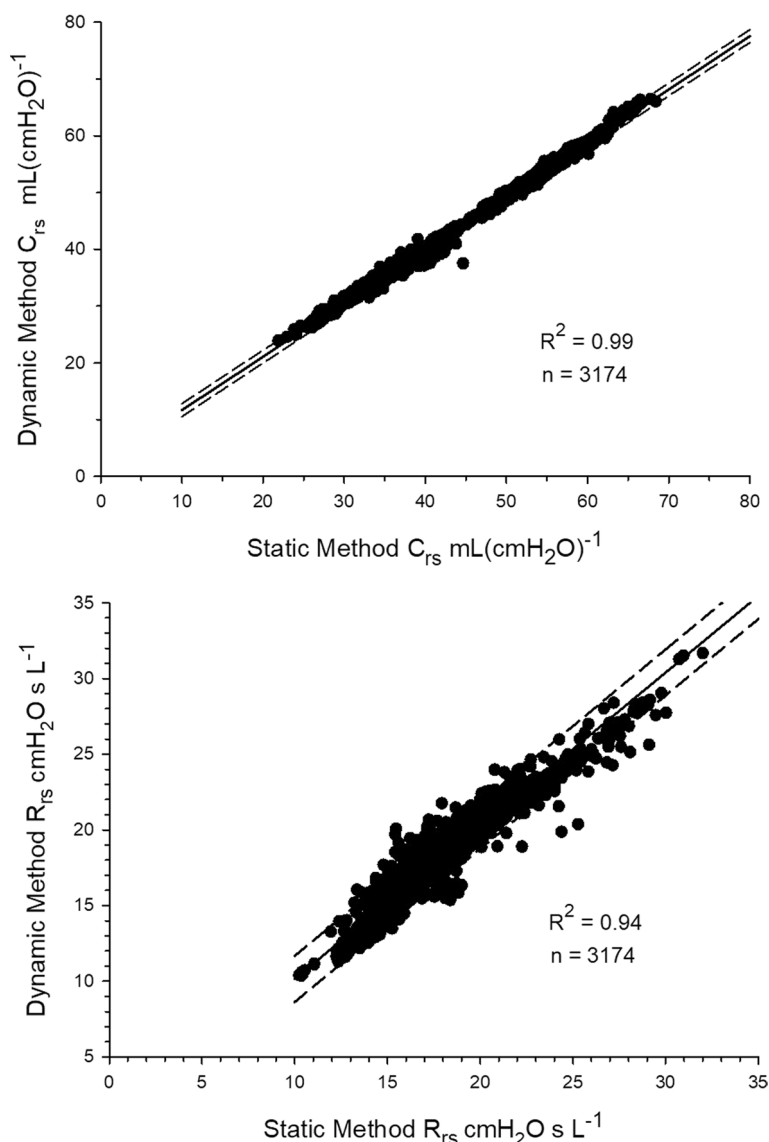


Fig. 3 Pearson's linear regression using data generated by the 15 patients in the study. Compared were average epoch measurements of C_{rs} and of R_{rs} by the static and dynamic methods ($n = 3174$). $(C_{rs})_{stat} = 1.06 (C_{rs})_{dyn} - 2.26$; $R^2 = 0.99$; $p < 0.001$ and $(R_{rs})_{stat} = 0.93 (R_{rs})_{dyn} + 1.02$; $R^2 = 0.94$; $p < 0.001$

conditions [22]. It should be noted that the one-compartment model of Otis et al. [7] does not allow for the partitioning of respiratory system mechanics. On the other hand, a similar numerical approach may be considered when solving a more complex model of the respiratory system, one that accounts for both lung and chest wall compliances.

Method validation was done with matching pairs of C_{rs} and R_{rs} calculated by the static and the dynamic methods. Experimental method validation yielded nearly identical C_{rs} and R_{rs} values when tested with a test lung ventilated using different V_{tidal} and applied PEEP levels. Since C_{rs} and R_{rs} were more or less fixed for the test lung, the dynamic method also was validated using airway signals from a previous study on mechanically ventilated patients. The use of clinical data yielded a more realistic assessment of the dynamic method, allowing for method comparison at C_{rs} values

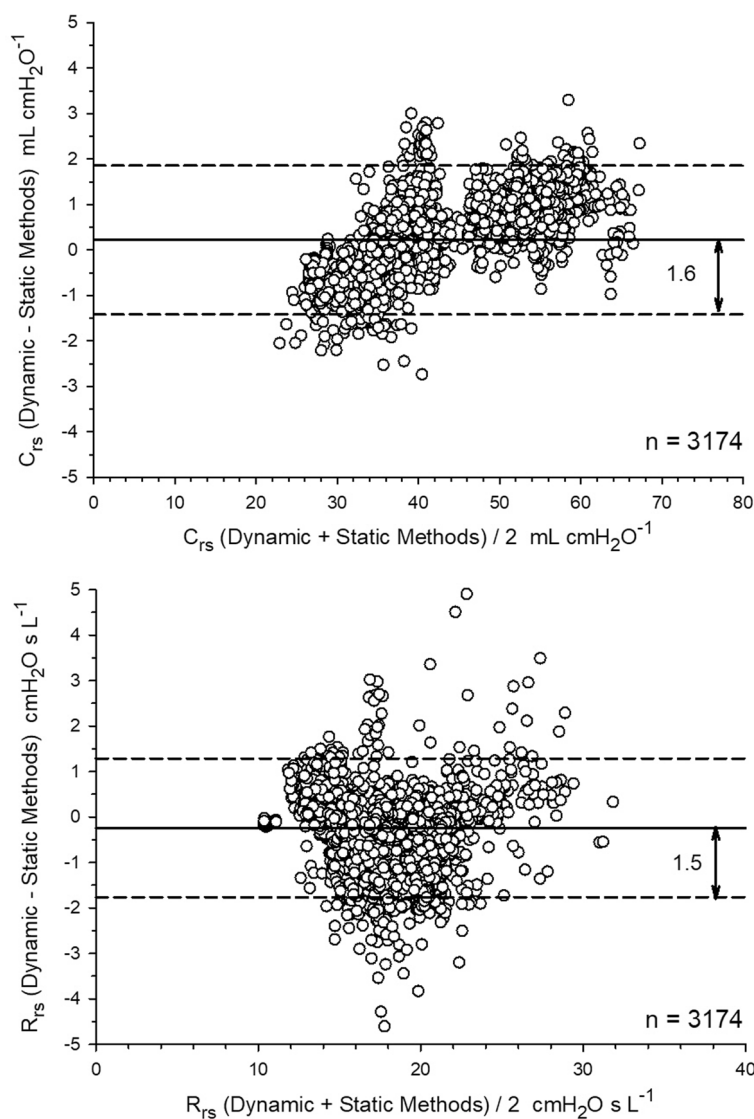


Fig. 4 Bland–Altman analysis of average epoch measurements of C_{rs} and R_{rs} ($n = 3174$) from the data generated by the 15 patients in the study. Bias \pm 95% LOA was 0.2 ± 1.6 mL·cmH₂O⁻¹ for C_{rs} and -0.2 ± 1.5 cmH₂O·s·L⁻¹ for R_{rs}

ranging from 20 to 70 mL·cmH₂O⁻¹ and from 10 to 32 cmH₂O·s·L⁻¹ for R_{rs} . These are ranges similar to those encountered in clinical practice.

Software was written to identify breaths meeting strict morphologic criteria that included a discernible plateau pressure and negligible P_{mus} or PEEP_i. This resulted in the evaluation of a massive number of individual breaths (78,371) contained in the 3174 identified epochs. The software calculated paired C_{rs} and R_{rs} values by the static and dynamic methods in all identified breaths enclosed within each 131.1-s-long epoch, reporting the epoch’s average for comparison. The use of epochs was dictated both by the format initially used to store the data and by the ability to assess respiratory muscle activity indirectly by spectral analysis.

Table 2 Bland–Altman analysis of respiratory system's static compliance and resistance values calculated by the static and dynamic methods for individual patients

| Patient | Epochs (3174) | Breaths (78,371) | Compliance mL·cmH ₂ O ⁻¹ | | | Resistance cmH ₂ O·s·L ⁻¹ | | |
|---------|------------------|---------------------|--|--------------|------------|---|--------------|------------|
| | | | Mean value | Bias | LOA | Mean value | Bias | LOA |
| 1 | 293 | 5924 | 35.8 | 0.4 | 1.1 | 21.9 | 0.4 | 1.4 |
| 2 | 119 | 4917 | 27.5 | − 0.6 | 0.9 | 15.2 | 0.2 | 2.2 |
| 3 | 127 | 2926 | 58.6 | 1.4 | 0.9 | 14.3 | 0.2 | 0.3 |
| 4 | 385 | 8632 | 32.8 | − 0.3 | 1.2 | 20.5 | − 0.3 | 0.9 |
| 5 | 15 | 459 | 59.7 | 1.6 | 0.9 | 16.7 | − 0.1 | 0.6 |
| 6 | 38 | 660 | 46.7 | 1.6 | 2.3 | 13.6 | − 0.4 | 1.9 |
| 7 | 399 | 11,714 | 39.7 | 0.2 | 0.9 | 15.4 | 0.1 | 1.1 |
| 8 | 881 | 17,953 | 53.5 | 0.8 | 0.8 | 16.8 | − 0.3 | 0.6 |
| 9 | 72 | 1718 | 49.7 | 1.3 | 0.8 | 17.7 | − 0.1 | 0.5 |
| 10 | 27 | 426 | 41.2 | 1.4 | 1.3 | 17.4 | 2.1 | 1.1 |
| 11 | 38 | 1123 | 47.5 | 0.7 | 1.1 | 12.2 | 0.8 | 0.4 |
| 12 | 26 | 494 | 52.5 | 0.0 | 0.7 | 12.0 | − 0.1 | 0.2 |
| 13 | 248 | 6771 | 34.8 | − 0.8 | 0.7 | 18.9 | − 1.6 | 0.8 |
| 14 | 476 | 14,067 | 33.8 | − 0.5 | 1.2 | 15.6 | − 0.5 | 1.6 |
| 15 | 30 | 587 | 64.7 | 0.6 | 1.3 | 12.9 | 0.2 | 0.3 |
| Median | 119 | 2926 | 46.7 | 0.6 | 0.9 | 15.6 | − 0.1 | 0.8 |
| IQR | [34,339] | [624,7702] | [35.3, 53.0] | [− 0.2, 1.4] | [0.8, 1.2] | [13.9, 17.5] | [− 0.3, 0.2] | [0.5, 1.2] |

Mean value = average value of all measurements used in the Bland–Altman analysis; LOA = 95% limits of agreement; IQR = interquartile range]

The cohort was composed mainly of highly sedated patients transferred from the Emergency Department and ventilated with end-inspiratory holds that were not immediately detected by the ICU team. Although the data were collected several years ago, neither the passage of time nor changes in ICU care should have influenced the results presented nor adversely altered the fidelity of the stored airway signals.

To provide for a balanced assessment of the data, analysis was performed in aggregate form and also individually for each patient in the study. Whereas aggregate analysis biased the results in favor of patients with many analyzed epochs, individual analysis amplified the effect of patients with fewer epochs. Regardless of comparison strategy, however, both methods produced nearly identical C_{rs} and R_{rs} values with negligible bias and exceedingly small LOA.

Although method bias was minimal for both C_{rs} and R_{rs} , the possibility should be acknowledged of introducing a systematic error by the software when calculating the “gold standards” C_{rs} and R_{rs} by the static method. The cessation of gas flow during the end-inspiratory hold produces a rapid decline in P_{aw} from P_{peak} to P_1 , followed by a slow decay to a plateau P_2 [23]. The timing of the end-inspiratory hold (t_{hold}) could be an important source of measurement error since a short t_{hold} may affect P_1 by the persistence of airflow during inspiratory valve closure or P_2 by prematurely shortening the decay of P_{aw} . Conversely, a long t_{hold} may allow voluntary respiratory muscle activity to occur, also distorting P_2 . All breaths in the study were ventilator triggered with no evidence of spontaneous respiratory muscle activity throughout the length of the breath, including the end-inspiratory hold portion. For the cohort, t_{hold} was 0.4 [0.4,0.4] (range 0.3 to 0.7) seconds, allowing ample time for inspiratory valve closing

[24] and placing P_2 firmly on the flat portion of the plateau, as evidenced by the small decline in P_{aw} (< 1.0 cmH₂O) predicted by decreasing exponentials fitted to the data ($R^2 = 0.96$) and extrapolated from 0.4 to 1.0 s (Additional file 1: Section S4).

Several assumptions were made in the development of the dynamic method, among them the constancy of C_{rs} and R_{rs} during insufflation. This basic tenet of the one-dimensional model of Otis et al. [7] is unlikely to hold true during the early stages of inspiration where the volume signal is curvilinear [23]. Past a certain inflation volume, defined here as ΔV_{LIP} , C_{rs} becomes constant and remains so over the rest of the tidal range [25]. The dynamic method was therefore applied to insufflation lung volumes > 200 mL, a ΔV_{LIP} chosen to match those reported in ARDS patients [26, 27]. This is probably a conservative estimate since no patient in the study met the Berlin definition for ARDS [28] with half the cohort having normal chest radiographs. Moreover, all patients were ventilated with $PEEP_a = 5$ cmH₂O, likely resulting in initial lung volumes in the region of constant C_{rs} . It is possible, however, that small variations in C_{rs} and R_{rs} during the studied insufflation volumes resulted in the slight uncertainty noted in determining the intersection of the $C_{rs} - R_{rs}$ functions.

The assumption of absent patient inspiratory effort during insufflation ($P_{mus} = 0$) cannot be independently verified since esophageal balloon catheters were not used in the original study. The validity of this assumption rests on: (1) the use of $RRV < 55\%$ as an inclusion criterion, a value noted in heavily sedated ventilated patients [29] and normal individuals during stages of deep sleep; (2) all analyzed breaths were ventilator-initiated; and (3) a cohort of 50 epochs selected randomly from the sample population was characterized by a regular breathing pattern, low respiratory rate (11 [11, 14] bpm) and no signal distortion (see Additional file 1: Section S7 and Table 2e).

The assumption of absent $PEEP_i$ also could not be independently verified, but care was taken to include in the analysis only breaths displaying minimal differences between its onset and the prior breath's end-exhalation F_{aw} and P_{aw} . In addition, (1) no patient in the study was diagnosed with obstructive lung disease; (2) the exhalation time for the cohort allowed ample time for expiration (3.2 ± 0.7 s); and (3) tachypnea ($RR > 20$ bpm) was absent in all chosen epochs.

The dynamic method is unlikely to perform well under conditions of persistent asynchronous breathing or in the presence of significant respiratory muscle effort. It is also not amenable for bedside use or with ventilators lacking airway signal sampling. Conversely, when used in conjunction with a computer connected to the ventilator's data-port, the dynamic method may provide accurate ongoing measurements of C_{rs} and R_{rs} under most clinical conditions encountered during the provision of volume-controlled mechanical ventilation.

Although the present study was not intended as a methodological comparison, the dynamic method appears to perform as well or better than either the LSF or the τ_e methods (Additional file 1: Table S3). Unlike these empirical models, the dynamic method represents a deterministic approach to the solution of the equation of motion. As such, it may be applicable to ventilatory modes other than VC and provide insight into the relationship of respiratory system mechanics to other ventilatory variables, such as plateau pressure, respiratory muscle effort and intrinsic PEEP. These, and other issues related to the application of the dynamic method await further confirmation by prospective studies.

Take-home message

A novel numerical method to calculate static compliance and airway resistance of the respiratory system during ventilatory support is developed and validated.

Abbreviations

| | |
|-------------------|--|
| C_{rs} | Respiratory system static compliance |
| ΔV | Lung volume change during insufflation |
| ΔV_{LIP} | Lung volume at the lower inflection point |
| ΔV_{UIP} | Lung volume at the upper inflection point |
| DC | Flow spectrum zero frequency component amplitude |
| F_{aw} | Airway flow |
| FFT | Fast Fourier transform algorithm |
| H1 | First harmonic amplitude of the flow or pressure signal spectrum |
| I | Inertia of the respiratory system |
| LIP | Lower inflection point |
| LOA | 95% Limits of agreement |
| LSF | Multiple least squares fit |
| P_{aw} | Airway pressure |
| PEEP _a | Applied positive end expiratory pressure |
| PEEP _i | Intrinsic PEEP present at end expiration |
| P_{mus} | Respiratory muscles applied pressure |
| P_{peak} | Peak inspiratory pressure |
| $P_{plateau}$ | Plateau pressure during the end-inspiratory hold |
| P_{vent} | Ventilator applied pressure |
| rs | Respiratory system |
| R_{rs} | Respiratory system airway resistance |
| RRV | Respiratory rate variability |
| te | Expiratory time constant |
| T_{hold} | Timing of the expiratory hold |
| t_k | A point in time during insufflation |
| UIP | Upper inflection point |
| VC | Volume controlled |
| $V(t)$ | Lung volume as a function of time |
| V_{tidal} | Tidal volume |

Supplementary Information

The online version contains supplementary material available at <https://doi.org/10.1186/s40635-022-00483-2>.

Additional file 1: Table S1. Demographic and ICU Admission Data, Diagnoses, and ICU Admission Chest X Rays for Study Patients. **Table S2.** Average Ventilatory Parameters Computed from All Epochs Used in Method Comparison. **Table S3.** Comparison of bias \pm Limits of Agreement (LOA) for C_{rs} and R_{rs} calculated From Individual Patient Data by the Dynamic, Least Square Fitting (LSF) and Expiratory Time Constant (τ_e) Methods.

Additional file 2. Fitting double exponential.

Additional file 3. Raw data individual and aggregate.

Additional file 4. Experimental data results.

Acknowledgements

The author thanks the Commission for Educational Exchange between the United States, Belgium and Luxembourg and the Fulbright Scholarship Board for their generous support as a Fulbright Research Scholar at the Erasme Hospital of the Université Libre de Bruxelles.

Author contributions

The author read and approved the final manuscript.

Funding

Not applicable.

Availability of data and materials

The datasets used and analyzed during the current study can be found in the Electronic Data Repository. The database storing the raw data is available from the author upon reasonable request.

Declarations

Ethics approval and consent to participate

The database used in the present study was collected in 2011 as part of research on respiratory rate variability (Gutierrez et al., *Intensive Care Med.* 2013; 39:1359–1367). The study was approved by The George Washington University IRB (IRB No. 110910) that allowed use of the deidentified data in further studies.

Consent for publication

Not applicable.

Competing interests

The author has applied for a U.S. patent based on the information presented in the paper.

Received: 17 August 2022 Accepted: 17 December 2022

Published online: 30 December 2022

References

- D'Angelo E, Calderini E, Torri G, Robatto FM, Bono D, Milic-Emili J (1989) Respiratory mechanics in anesthetized paralyzed humans: effects of flow, volume, and time. *J Appl Physiol* 67:2556–2564. <https://doi.org/10.1152/jappl.1989.67.6.2556>
- Bernasconi M, Ploysongsang Y, Gottfried SB, Milic-Emili J, Rossi A (1988) Respiratory compliance and resistance in mechanically ventilated patients with acute respiratory failure. *Intensive Care Med* 14:547–553. <https://doi.org/10.1007/BF00263528>
- Wald A, Jason D, Murphy TW, Mazzia VDB (1969) A computer system for respiratory parameters. *Comput Biomed Res* 2:411–429. [https://doi.org/10.1016/0010-4809\(69\)90007-x](https://doi.org/10.1016/0010-4809(69)90007-x)
- Uhl RR, Lewis FJ (1974) Digital computer calculation of human pulmonary mechanics using a least square fit technique. *Comput Biomed Res* 7:489–495. [https://doi.org/10.1016/0010-4809\(74\)90027-5](https://doi.org/10.1016/0010-4809(74)90027-5)
- Al-Rawas N, Banner MJ, Euliano NR, Tams CG, Brown J, Martin AD, Gabrielli A (2013) Expiratory time constant for determinations of plateau pressure, respiratory system compliance, and total resistance. *Crit Care* 17:R23. <https://doi.org/10.1186/cc12500>
- McIlroy MB, Tierney DF, Nadel JA (1963) A new method for measurement of compliance and resistance of the lungs and thorax. *J Appl Physiol* 17:424–427
- Otis AB, Fenn WO, Rahn H (1950) Mechanics of breathing in man. *J Appl Physiol* 2:592–607. <https://doi.org/10.1152/jappl.1950.2.11.592>
- Marini JJ (2011) Dynamic hyperinflation and auto-positive end-expiratory pressure: lessons learned over 30 years. *Am J Respir Crit Care Med* 184:756–762. <https://doi.org/10.1164/rccm.201102-0226PP>
- Mead J (1956) Measurement of inertia of the lungs at increased ambient pressure. *J Appl Physiol* 9:208–212. <https://doi.org/10.1152/jappl.1956.9.2.208>
- Prezant DJ, Aldrich TK, Karpel JP, Park SS (1990) Inspiratory flow dynamics during mechanical ventilation in patients with respiratory failure. *Am Rev Respir Dis* 142:1284–1287. https://doi.org/10.1164/ajrccm/142.6_Pt_1.1284
- Gutierrez G, Das A, Ballarino G, Beyzaei-Arani A, Türkan H, Wulf-Gutierrez M, Rider K, Kaya H, Amdur R (2013) Decreased respiratory rate variability during mechanical ventilation is associated with increased mortality. *Intensive Care Med* 39:1359–1367. <https://doi.org/10.1007/s00134-013-2937-5>. (Epub 2013 Jun 7)
- Gutierrez G, Ballarino GJ, Turkan H, Abril J, De La Cruz L, Edsall C et al (2011) Automatic detection of patient-ventilator asynchrony by spectral analysis of airway flow. *Crit Care* 15:R167. <https://doi.org/10.1186/cc10309>
- Duhamel P, Vetterli M (1990) Fast Fourier transforms: a tutorial review and a state of the art. *Signal Process* 19:259–299. [https://doi.org/10.1016/0165-1684\(90\)90158-U](https://doi.org/10.1016/0165-1684(90)90158-U)
- Gutierrez G, Williams J, Alrehaili GA, McLean A, Pirouz R, Amdur R et al (2016) Respiratory rate variability in sleeping adults without obstructive sleep apnea. *Physiol Rep* 4:e12949. <https://doi.org/10.14814/phy2.12949>
- Brochard L (2002) Intrinsic (or auto-) PEEP during controlled mechanical ventilation. *Intensive Care Med* 28:1376–1378. <https://doi.org/10.1007/s00134-002-1438-8>. (Epub 2002 Aug 17)
- Rossi A, Gottfried SB, Zocchi L, Higgs BD, Lennox S, Calverley PM, Begin P, Grassino A, Milic-Emili J (1985) Measurement of static compliance of the total respiratory system in patients with acute respiratory failure during mechanical ventilation. The effect of intrinsic positive end-expiratory pressure. *Am Rev Respir Dis* 131:672–677. <https://doi.org/10.1164/arrd.1985.131.5.672>
- Servillo G, Svantesson C, Beydon L, Roupie E, Brochard L, Lemaire F, Jonson B (1997) Pressure–volume curves in acute respiratory failure: automated low flow inflation versus occlusion. *Am J Respir Crit Care Med* 155:1629–1636. <https://doi.org/10.1164/ajrccm.155.5.9154868>
- Bland JM, Altman DG (1986) Statistical methods for assessing agreement between two methods of clinical measurement. *Lancet* 1:307–310
- Gutierrez G (2020) Artificial intelligence in the intensive care unit. *Crit Care* 24:101. <https://doi.org/10.1186/s13054-020-2785-y>
- Amato MB, Meade MO, Slutsky AS, Brochard L, Costa EL, Schoenfeld DA, Stewart TE, Briel M, Talmor D, Mercat A, Richard JC, Carvalho CR, Brower RG (2015) Driving pressure and survival in the acute respiratory distress syndrome. *N Engl J Med* 372:747–755. <https://doi.org/10.1056/NEJMs1410639>
- Rossi A, Gottfried SB, Higgs BD, Zocchi L, Grassino A, Milic-Emili J (1985) Respiratory mechanics in mechanically ventilated patients with respiratory failure. *J Appl Physiol* 58:1849–1858. <https://doi.org/10.1152/jappl.1985.58.6.1849>

22. Sharp JT, Henry JP, Sweany SK, Meadows WR, Pietras RJ (1964) Total respiratory inertance and its gas and tissue components in normal and obese men. *J Clin Invest* 43:503–509. <https://doi.org/10.1172/JCI104936>
23. Bates JH, Baconnier P, Milic-Emili J (1988) (1985) A theoretical analysis of interrupter technique for measuring respiratory mechanics. *J Appl Physiol* 64:2204–2214. <https://doi.org/10.1152/jappl.1988.64.5.2204>
24. Bates JH, Hunter IW, Sly PD, Okubo S, Filiatrault S, Milic-Emili J (1987) Effect of valve closure time on the determination of respiratory resistance by flow interruption. *Med Biol Eng Comput* 25:136–140. <https://doi.org/10.1007/BF02442841>
25. Truwit JD, Marini JJ (1988) Evaluation of thoracic mechanics in the ventilated patient part II: applied mechanics. *J Crit Care* 3:199–213. [https://doi.org/10.1016/0883-9441\(88\)90092-5](https://doi.org/10.1016/0883-9441(88)90092-5)
26. Mergoni M, Volpi A, Bricchi C, Rossi A (2001) (1985) Lower inflection point and recruitment with PEEP in ventilated patients with acute respiratory failure. *J Appl Physiol* 91:441–450. <https://doi.org/10.1152/jappl.2001.91.1.441>
27. Ward NS, Lin DY, Nelson DL, Houtchens J, Schwartz WA, Klinger JR et al (2002) Successful determination of lower inflection point and maximal compliance in a population of patients with acute respiratory distress syndrome. *Crit Care Med* 30:963–968. <https://doi.org/10.1097/00003246-200205000-00002>
28. Definition Task Force ARDS, Ranieri VM, Rubenfeld GD, Thompson BT, Ferguson ND, Caldwell E, Fan E, Camporota L, Slutsky AS (2012) Acute respiratory distress syndrome: the Berlin Definition. *JAMA* 307:2526–2533. <https://doi.org/10.1001/jama.2012.5669>
29. Turkan H, Kaya H, Rider K, Wulf-Gutierrez M, Gutierrez G (2014) Mean Bispectral (BIS) values and patient-ventilator synchrony correlate with Richmond Agitation Sedation Scale (RASS) in sedated patients. *Amer J Respir Crit Care Med* 189:A3940

Publisher's Note

Springer Nature remains neutral with regard to jurisdictional claims in published maps and institutional affiliations.

Submit your manuscript to a SpringerOpen[®] journal and benefit from:

- Convenient online submission
- Rigorous peer review
- Open access: articles freely available online
- High visibility within the field
- Retaining the copyright to your article

Submit your next manuscript at ► [springeropen.com](https://www.springeropen.com)
